Journal of Alloys and Compounds 722 (2017) 83–87

Contents lists available at ScienceDirect

Journal of Alloys and Compounds

journal homepage: http://www.elsevier.com/locate/jalcom

Magnetic field annealing effect and superparamagnetic contributions in one-dimensional CoPt nanostructures

S.S. Ali [a, b], W.J. Li [a], K. Javed [a], M. Irfan [a], Fazal-e-Aleem [b], G.J. Zhai [c], X.F. Han [a, *]

[a] Institute of Physics, Chinese Academy of Sciences, Beijing 100190, China
[b] Department of Physics, The University of Lahore, Lahore 54000, Pakistan
[c] National Space Science Center, Chinese Academy of Sciences, Beijing 100190, China

ARTICLE INFO

Article history:
Received 6 February 2017
Received in revised form
28 May 2017
Accepted 5 June 2017
Available online 8 June 2017

Keywords:
Electrodeposition
Nanowires

ABSTRACT

A low cost versatile electrochemical method has been employed to synthesize highly ordered CoPt nanowires (NWs) in anodic aluminum oxide (AAO) templates with average pore diameter of about 100 nm. The structural properties of as deposited NWs have been studied through XRD analysis showing face centered cubic (fcc) as the dominant phase of CoPt NWs. Magnetic properties at room temperature and lower temperature has been investigated with applied field parallel and perpendicular to NWs axis. The easy magnetization axis is aligned perpendicular to NWs owing to the strong magnetostatic interactions among the NWs due to smaller interwire distance (~15 nm). Furthermore, the as deposited arrays of NWs have been annealed for 2 h at 300 °C in the presence of 1 T magnetic field applied in the direction perpendicular to NWs axis. Magnetic field annealing gives improved structural and magnetic behavior of these one-dimensional (1D) nanostructures resulting improved crystallinity and increased values of coercivity (H_c) and remnant squareness (SQ). Superparamagnetic contributions at lower temperature due to presence of fine nanoparticles in blocking state play important role and leads to enhanced magnetic behavior of CoPt NWs.

1. Introduction

Several important applications in the field of electronics, photonics, catalysis information storage, optical sensing, biological labeling and surface-enhanced Raman scattering studies are associated with the synthesis and investigation of nanostructural materials. At submicron level the geometrical shape of nanostructure plays crucial role regarding their practical implementation owing to the influence of anisotropy. Particularly, metallic nanowires (NWs) are of much consideration because of their unique magnetic properties and potential technological application against their bulk counterparts [1–5]. One dimensional (1D) magnetic nanostructure specifically magnetic NWs arrays have specially been studied regarding potential applications in high-density perpendicular magnetic recording media [6]. Magnetically isolated grains of less than 10 nm in diameter with high magnetocrystalline anisotropy are required for higher magnetic recording density with low noise. Meeting this requirement inhibits thermal fluctuations that tend to destabilize the magnetization of the recorded bits [7]. Superparamagnetism comes into effect when reaching the ultrahigh density magnetic recording with 1 bit down to nanosize. This problem can be fixed possibly by either to increase the effective anisotropy of material or to increase the nanostructure dimensions from nanodots to nanocylinders (nanowires and nanotubes) [8,9]. A lot of research has been devoted to achieve the combined goals of high recording density of bits with enough stability [10–12]. The template assisted fabrication technique of 1D magnetic NWs is of particular importance specially because the synthesized nanostructures from this method are well erected and comprise of highly ordered patterns of magnetically isolated units [13–15]. Aluminum anodizing technology has been developed to such a degree that the dimensions and distribution of pores in the film can be artificially controlled by preindentation. The anodic aluminum oxide (AAO) templates have the advantages of chemical stability and easy control of nano-channels' diameter and density [16]. Electrochemical deposition of transition metals and their alloys into nano-channels of AAO templates is a low cost and versatile method to synthesize magnetic NWs and NTs of tunable length and diameter with high aspect ratio [17,18]. A

* Corresponding author.
E-mail address: xfhan@iphy.ac.cn (X.F. Han).

http://dx.doi.org/10.1016/j.jallcom.2017.06.073
0925-8388/

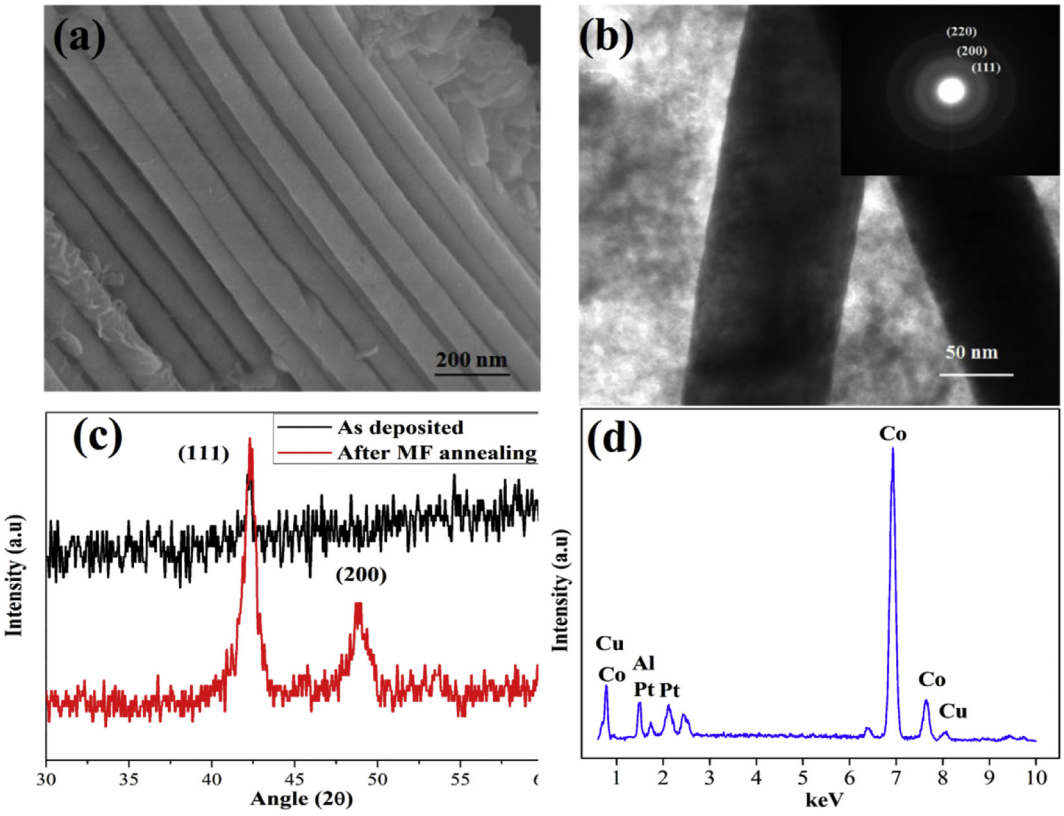

Fig. 1. (a) SEM image of CoPt nanowires with average diameter of about 100 nm after partial etching in NaOH solution. (b) TEM image of CoPt nanowires after complete removel of AAO template, inset shows SAED pattern. (c) XRD pattern of as deposited and annealed CoPt nanowires showing fcc phase with (111) preferred orientation. (d) EDX spectrum showing the deposition of Co and Pt contents.

number of magnetic nanostructures including Fe, Co, Ni and their alloys Fe–Co and Fe–Ni have been efficiently prepared by electrodeposition [19–25]. The microstructure grain size and crystalline orientation of deposits play important role to affect the magnetic characteristics such as saturation magnetization (M_s), coercivity (H_c) and remanent magnetization (M_r). These properties are even further dependent on the conditions under which deposits are prepared and treated [26,27].

2. Experiments

Well ordered CoPt NWs with average diameter of 100 nm have been electrochemically deposited into AAO templates with a constant stirring during electrodeposition process. The thickness of AAO template is about 60 μm and the pore density is 1×10^9 pores cm^{-2}. Before electrodeposition a 200 nm Cu layer has been sputtered at one side of AAO template to serve as conducting electrode. The electrolyte composed of 0.1 M cobalt sulfamate, 0.1 M diamminedinitritoplatinum, and 0.15 M diammonium hydrogen citrate has been used for electrochemical deposition with pH around 3.5 [28]. A three electrode cell has been employed in constant voltage mode at room temperature to get a continuous growth process. Magnetic field annealing has been done with field direction perpendicular to NWs axis and strength of 1 T at temperature of 300 °C for 2 h. For x-ray diffraction (XRD) analysis RIGAKU D/MAX-2400 has been employed with radiation CuKα and the wavelength is 1.5405 Å. The morphology of CoPt NWs has been investigated by high resolution scanning electron microscope (SEM; Hitachi S-4800 operated at an accelerating voltage of 10 kV) and transmission electron microscope (TEM; JEOL 2011 with an accelerating voltage of 200 kV). Before SEM analysis the AAO template has been partially etched in 1 M NaOH solution but for TEM analysis it is necessary to remove the template completely to get the NWs liberated from the template, thus etching in the same solution as mentioned above has been done at 60 °C for about 12 h. Vibrating sample magnetometer (VSM; Microsense EV-9) has been employed at RT for magnetic hysteresis curves (M-H loops) measurements and superconducting quantum interference device (SQUID) at lower temperatures.

3. Results and discussions

Fig. 1(a) shows the scanning electron microscope image of well ordered CoPt NWs of 100 nm diameter after partial removel of AAO template. Owing to the controlled growth process and use of AAO templates the wires are well aligned and the dimensions are controlled by choosing the desired pore diameter in AAO template and the elecrodeposition time to tune the length. Fig. 1(b) shows the TEM image of CoPt NWs after being etched for several hours resulting complete removel of AAO template. Fig. 1(c) shows the XRD pattern of as deposited NWs and the ones annealed in magnetic field illustrating them textured along the face centered cubic (fcc) phase with (111) preferred orientation. The JCPDS card 04-003-3912 has been used to index the XRD pattern. It can be seen in XRD patterns that after magnetic field annealing with magnetic field applied perpendicular to NWs axis, which is also the easy magnetization axis, the peak sharpness increases significantly showing better crystallinity. This improved crystalline structure after magnetic field annealing is attributed to the alignment of more crystalline grains along the applied field direction. Fig. 1(d)

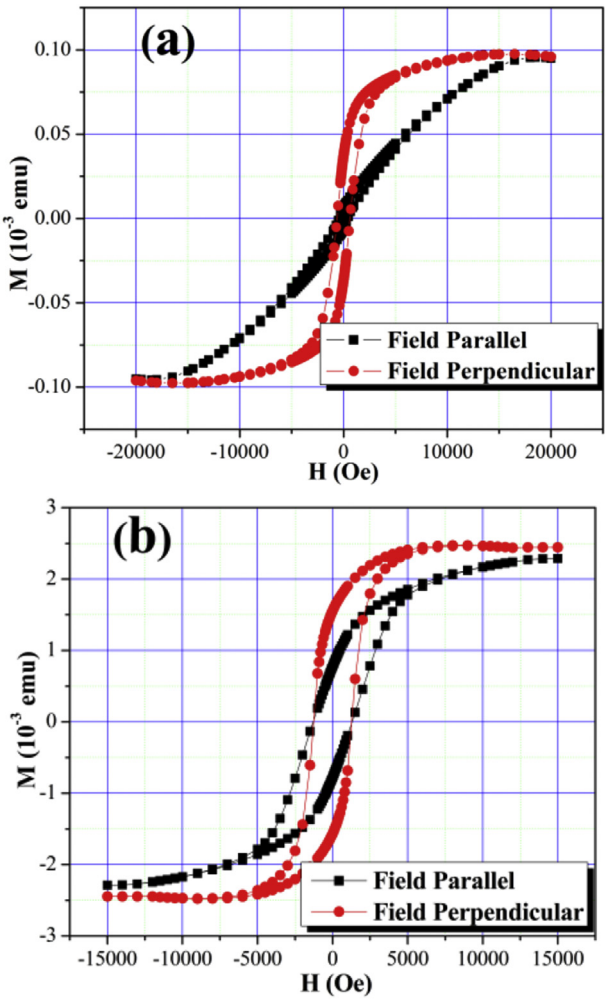

Fig. 2. M-H hysteresis loops of CoPt NWs (a) as deposited (b) after magnetic field annealing at 300 °C for 2 h.

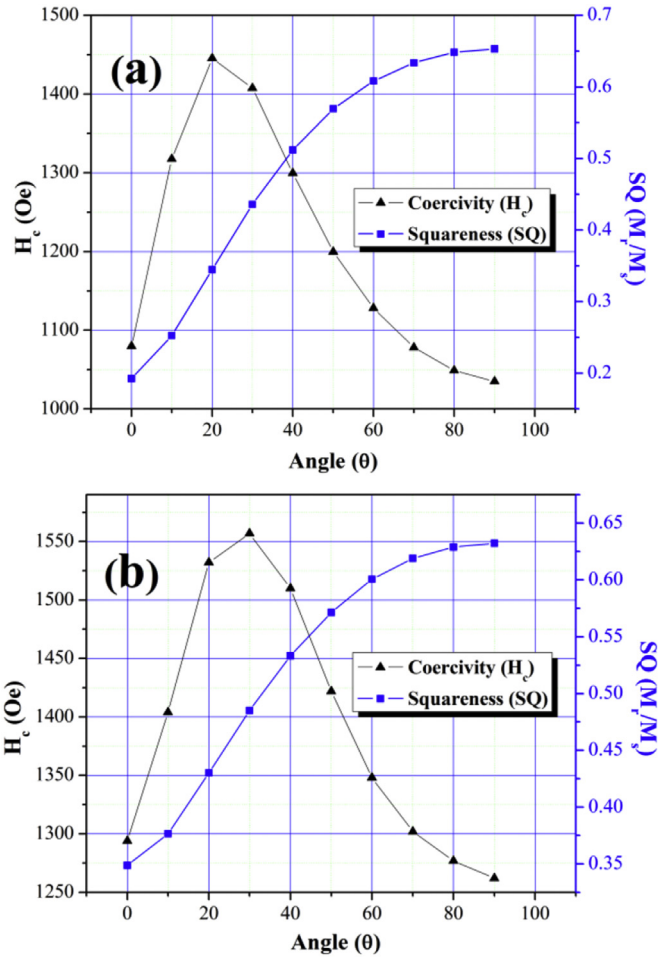

Fig. 3. Angular dependence of coercivity (H_c) and squareness (SQ) of (a) as deposited sample (b) after magnetic field annealing at 300 °C for 2 h.

shows the EDX spectrum of partially etched CoPt NWs confirming the deposition of Co and Pt contents. In this spectrum Cu peak is appeared due to the sputtered Cu layer at the bottom which served as conducting electrode during elecrodeposition and Al peak due to the partial etching of AAO template.

Fig. 2(a and b) shows the M-H hysteresis loops of as deposited and annealed CoPt NWs measured by VSM at RT. The magnetic field annealing has been employed with field direction perpendicular to NWs axis with strength of 1 T for 2 h. For both cases the perpendicularly aligned easy magnetization axis can been seen in Fig. 2(a and b). In our experiments the strong magnetostatic interactions among the NWs owing to the smaller interwire distance (~15 nm) tend to align the easy magnetization axis perpendicular to the NWs axis. The alignment of easy magnetization axis is dependent on effective anisotropy field (H_k). The shape anisotropy field ($2\pi M_s$), magnetostatic interaction field and the magnetocrystalline anisotropy (H_{ma}) are three major contributions in effective anisotropy field (H_k). The dominant behavior of shape anisotropy aligns the easy magnetization axis along the parallel direction of NWs axis whereas stronger magnetostatic interactions result the opposite case [29]. Since the easy magnetization axis is aligned perpendicular to NWs axis, therefore the annealing field applied in the direction of easy magnetization axis favors more crystalline grains to get aligned perpendicular to NWs axis.

The model of prolate ellipsoid chains gives a direct proportional relation between H_c and M_s given as:

$$H_c = \left[\pi(6M_n + 2L_n)a^2M_s \Big/ \left(6b^2\right)\right] + \left[4\pi\left(N_\perp - N_\parallel\right)M_s\right] \qquad (1)$$

where

$$M_n = \sum_{j=1}^{(n-2)/2<j\le n/2} (n-2j) \Big/ \left[n(2j)^3\right]$$

$$L_n = \sum_{j=1}^{(n-1)/2<j\le(n+1)/2} [n-(2j-1)] \Big/ \left[n(2j-1)^3\right]$$

In above equation n shows the number of ellipsoids in a single NW, being the length of short axis of ellipsoid a is equal to NW diameter as well, b is the length of long axis of ellipsoid and also equal to the distance between the centers of two ellipsoids, $N_\parallel$ and $N_\perp$ are demagnetization factors of the ellipsoid parallel and perpendicular to the NWs axis which depend on the aspect ratio of the ellipsoid. According to relation between H_c and M_s the increased value of M_s results increase in H_c as clear from above relation. Since the magnetic field direction during annealing process is perpendicular to NWs axis which is also the easy magnetization axis in our case due to strong magnetostatic interactions,

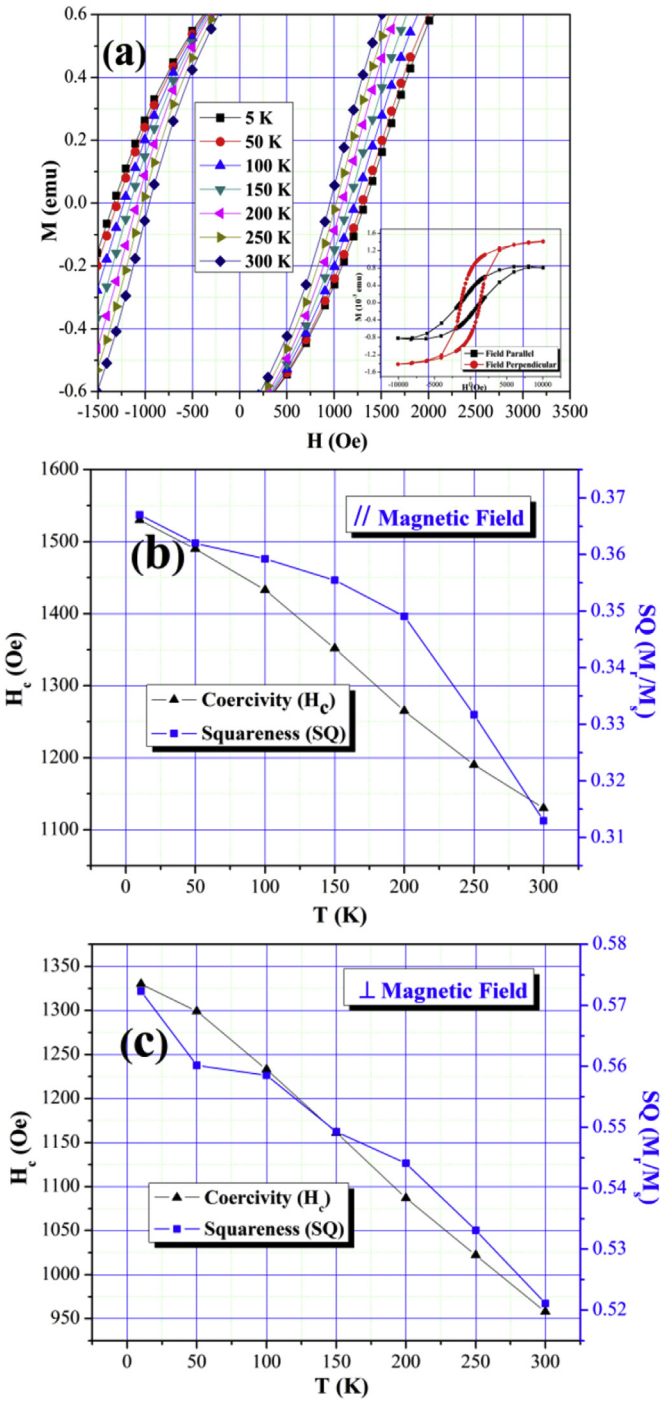

Fig. 4. (a) Magnified view of coercivity region in M-H hysteresis loop of CoPt NWs at 5 K, inset shows full M-H loop at 5 K. Temperature dependent variation in H_c and SQ with external field applied (b) parallel and (c) perpendicular to NWs axis.

therefore this field direction tends more magnetic moments to get aligned in the same direction leading to increased values of H_c as shown in Fig. 2(b). Owing to the magnetic field annealing the stress relief between grains and directional atomic pair ordering affected the magnetic features significantly [30]. This redistribution due to external magnetic field with heat treatment leads to a prominent increase in H_c from 1079 to 1294 Oe at $\theta = 0^\circ$ and the maximum value increased from 1447 to 1557 Oe.

Fig. 3(a) and (b) show the variation in H_c and SQ in CoPt NWs against the external magnetic field applied from $\theta = 0^\circ$ to $\theta = 90^\circ$ to NWs axis for as deposited and annealed samples respectively. The two important magnetization reversal mechanisms in NWs and NTs are the curling and coherent rotation modes. Increased values of H_c have been observed leading to a maximum of 1445 Oe at an angle of $\theta = 20^\circ$ for as deposited and 1557 Oe at angle of $\theta = 30^\circ$ for annealed samples where θ is the angle between applied magnetic field and NWs axis. This increase in H_c with the increase in the applied magnetic field angle corresponds to the curling mode of the magnetization reversal mechanism. At higher angles magnetization reversal mechanism has been switched from curling to coherent rotation mode showing a decrease in H_c values leading to a minimum at $\theta = 90^\circ$. The magnetization reversal mechanisms are mainly dependent on competition between exchange energy and demagnetization energy. According to the curling model, the coherent mode can be dominant due to increase in exchange energy density as there will be an increase in the relative angle between neighboring moments. Another reason which supports the dominant curling rotation is the increase in demagnetization energy density with the increase in the aspect ratio. This increase in demagnetization energy is possibly due to a magnetization component along the hard axis. Furthermore, formation of smaller domains is expected with the increase of aspect ratio, this in turn introduces additional domain walls with a corresponding increase in demagnetization energy [31]. To study the temperature dependent magnetic properties of CoPt NWs, M – H hysteresis curves have been taken by using superconducting quantum interference device (SQUID) at temperatures T = 5, 50, 100, 150, 200, 250 and 300 K with magnetic field applied parallel and perpendicular to the NW axis. Fig. 4(a) shows the magnified view of coercivity region when the field is applied in perpendicular direction and the inset shows the full M – H loop for both directions of external magnetic field at 5 K. Saturation magnetization (M_s) is increased up to 1.45 emu for perpendicular field and about 0.82 emu for parallel field. The increase in M_s in perpendicular direction of applied magnetic field is larger due to the alignment of easy magnetization axis in perpendicular direction. The overall increase in M_s is attributed to the reduced thermal fluctuations at lower temperatures which cause significant contributions to surface magnetic moments resulting in enhanced magnetic behavior. Fig. 4 (b,c) shows the temperature dependent behavior of H_c and squareness (SQ) at lower temperatures up to 5 K. In both cases of applied field increase in H_c values up to 1530 and 1330 Oe (for//and ⊥ field respectively) and SQ values up to 0.36 and 0.57 (for//and ⊥ field respectively) has been observed with the decrease in temperature. Since the synthesis method in our case is electrodeposition in which there is a possibility of presence of fine nanoparticles in our samples at submicron level. At room temperature effectively these particles are in superparamagnetic state and do not contribute a net magnetization to the sample. While measuring magnetic properties employing SQUID at sufficiently low temperatures these nanoparticles are in blocking state and efficiently contribute to give enhanced H_c and SQ values. At lower temperatures the thermal relaxation over the anisotropy energy barrier gives additional increase in H_c [32].

4. Conclusions

In summary, CoPt NWs having 100 nm diameter have been synthesized by low cost electrochemical deposition method. The as deposited NWs are found to be textured along the face centered cubic (fcc) phase with (111) preferred orientation. Magnetic field annealing treatment to as deposited NWs improved the crystalline structure resulting a sharper (111) peak and improved (200) orientation. In this work significantly increased magnetic features

i.e. H_c from 1079 to 1294 Oe and SQ from 0.19 to 0.35 at $\theta = 0^\circ$ have been observed owing to heat treatment in the presence of 1 T magnetic field applied in the direction of easy magnetization axis. Out of three major contributions to effective anisotropy field (H_k), the strong magnetostatic interactions aligned the easy magnetization axis perpendicular to NWs. Switching in magnetization reversal mechanism has been observed from curling to coherent rotation for both cases which is quite interesting to study the mixed behavior of magnetic domains on applied field reversal. Furthermore, at lower temperatures significant increase in saturation magnetization, coercivity and squareness has been observed which is mainly due to the reduced thermal fluctuations and contribution of superparamagnetic nanoparticles in blocking state.

Acknowledgements

This work is supported by the State Key Project of Fundamental Research of Ministry of Science and Technology [MOST, No. 2010CB934400] National Natural Science Foundation [NSFC, Grant Nos. 11374351 and 11434014] and by Pakistan Higher Education Commission (HEC).

References

[1] N.L. Rosi, D.A. Giljohann, C.S. Thaxton, A.K.R. Lytton-Jean, M.S. Han, C.A. Mirkin, Science 312 (2006) 1027.
[2] S. Kang, J.W. Harrell, D.E. Nikles, Nano Lett. 2 (2002) 1033.
[3] A. Kros, R.J.M. Nolte, N.A.J.M. Sommerdijk, Adv. Mater. 14 (2002) 1779.
[4] R.C. Che, L.M. Peng, X.F. Duan, Q. Chen, X.L. Liang, Adv. Mater. 16 (2004) 401.
[5] R. Gasparac, P. Kohli, M.O. Mota, L. Trofin, C.R. Martin, Nano Lett. 4 (2004) 513.
[6] D.J. Sellmyer, M. Zheng, R. Skomski, J. Phys. Condens. Matter 13 (2001) R433.
[7] C. Tsang, M.M. Chen, T. Yogi, Proc. IEEE 81 (1993) 1346.
[8] S. Shamaila, D.P. Liu, R. Sharif, J.Y. Chen, H.R. Liu, X.F. Han, Appl. Phys. Lett. 94 (2009) 203101.
[9] M. Albrecht, A. Moser, C.T. Rettner, S. Anders, T. Thomson, B.D. Terris, Appl. Phys. Lett. 80 (2002) 3409.
[10] D.Y. Oh, J.K. Park, J. Appl. Phys. 93 (2003) 7756.
[11] M. Yu, Y. Liu, D.J. Sellmyer, J. Appl. Phys. 87 (2000) 6959.
[12] J.A. Christodoulides, Y. Huang, Y. Zhang, G.C. Hadjipanayis, I. Pana-giotopoulos, D. Niarchos, J. Appl. Phys. 87 (2000) 6938.
[13] Y.W. Wang, L.D. Zhang, G.W. Meng, X.S. Peng, Y.X. Jin, J. Zhang, J. Phys. Chem. B 106 (2002) 2502.
[14] Y. Peng, T.H. Shen, B. Ashworth, J. Appl. Phys. 93 (2003) 7050.
[15] R. Ferré, K. Ounadjela, J.M. George, L. Piraux, S. Dubois, Phys. Rev. B 56 (1997) 14066.
[16] S. Zhao, H. Roberge, A. Yelon, T.J. Veres, Am. Chem. Soc. 128 (2006) 12352.
[17] X.Y. Zhang, G.H. Wen, Y.F. Chan, R.K. Zheng, X.X. Zhang, N. Wang, Appl. Phys. Lett. 83 (2003) 3341.
[18] D.H. Qin, L. Cao, Q.Y. Sun, Y. Huang, H.L. Li, Chem. Phys. Lett. 35 (2002) 8484.
[19] Y. Peng, H.L. Zhang, S.L. Pan, H.L. Li, J. Appl. Phys. 87 (1999) 7405.
[20] Z.Y. Chen, Q.F. Zhan, D.S. Xue, F.S. Li, H. Kunkel, G. Williams, J. Phys. Condens. Matter 14 (2002) 613.
[21] X.Y. Zhang, G.H. Wen, Y.F. Chan, R.K. Zheng, X.X. Zhang, N. Wang, Appl. Phys. Lett. 83 (2003) 3341.
[22] R. Skomski, H. Zeng, M. Zheng, D.J. Sellmyer, Phys. Rev. B 62 (2000) 3900.
[23] L. Sun, P.C. Searson, C.L. Chien, Phys. Rev. B 61 (2000) R6463.
[24] Q.F. Zhan, Z.Y. Chen, D.S. Xue, F.S. Li, H. Kunkel, X.Z. Zhou, R. Roshko, G. Williams, Phys. Rev. B 66 (2002) 134436.
[25] Q.F. Liu, C.X. Gao, J.J. Xiao, D.S. Xue, J. Magn. Magn. Mater. 260 (2003) 151.
[26] S. Shamaila, R. Sharif, S. Riaz, M. Ma, M. Khaleeq-ur-Rahman, X.F. Han, J. Magn. Magn. Mater. 320 (2008) 1803.
[27] J. Mallet, K.Y. Zhang, S. Matefi-Tempfli, M. Matefi-Tempfli, L. Piraux, J. Phys. D 38 (2005) 909.
[28] F.M.F. Rhen, E. Backen, J.M.D. Coey, J. Appl. Phys. 97 (2005) 113908.
[29] G.C. Han, B.Y. Zong, P. Luo, Y.H. Wu, J. Appl. Phys. 93 (2003) 9202.
[30] S.S. Ali, K. Javed, D.W. Shi, L.L. Tao, J. Jiang, G.J. Zhai, X.F. Han, J. Appl. Phys. 115 (2014) 17A762.
[31] S.S. Ali, W.J. Li, K. Javed, D.W. Shi, S. Riaz, Y. Liu, Y.G. Zhao, G.J. Zhai, X.F. Han, Nanoscale 7 (2015) 13398.
[32] J.Y. Chen, N. Ahmad, D.W. Shi, W.P. Zhou, X.F. Han, J. Appl. Phys. 110 (2011) 073912.